Loss of CLDN5 in podocytes deregulates WIF1 to activate WNT signaling and contributes to kidney disease

Jie Yan
Binzhou Medical Univeristy
Hui Li
Qingdao University
Hui Sun
Hebei Medical University
Haotian Guo
Chinese Academy of Sciences
Jieying Liu
Binzhou Medical University
Mingxia Wang
Binzhou Medical University
Ninghua Lin
Binzhou Medical University
Xiangdong Wang
Binzhou Medical University
Xin Wang
Qingdao University
Li Li
Binzhou Medical University
Yongfeng Gong (ygong@bzmc.edu.cn)
Binzhou Medical Univeristy

Article

Keywords: kidney disease, WNT activity, CLDN5, WIF1

Posted Date: March 13th, 2021

DOI: https://doi.org/10.21203/rs.3.rs-285550/v1

Version of Record: A version of this preprint was published at Nature Communications on March 24th, 2022. See the published version at https://doi.org/10.1038/s41467-022-29277-6.

Abstract

Although mature podocytes lack tight junctions (TJs) and form slit diaphragms between opposing foot processes, TJ integral membrane protein CLDN5 is predominantly expressed throughout the plasma membrane of podocytes under normal conditions. Here using podocyte specific Cldn5 knockout mice as a model, we identify CLDN5 as a crucial regulator of podocyte function and reveal Cldn5 deletion exacerbates podocyte injury and proteinuria in diabetic nephropathy (DN) mouse model. Mechanistically, CLDN5 absence reduces ZO1 expression and induces the nuclear translocation of ZONAB, followed by transcriptional downregulation of WIF1, which leads to activation of WNT signaling pathway. Knockout Wif1 in podocytes result in the development of proteinuria and typical glomerular ultrastructure change occurring in Cldn5 knockout mice, while targeted delivery of Wif1 to podocytes prevents the development of glomerular nephropathy in Cldn5 knockout diabetic mice. Podocyte-derived WIF1 also plays a paracrine role on tubular epithelial cells, evidenced by animals with podocyte deletion of Cldn5 or Wif1 have worse kidney fibrosis after unilateral ureteral obstruction when compared with littermate controls with intact podocyte WIF1 expression. These findings establish a novel function of podocyte CLDN5 in restricting WNT activity in the kidney.

Introduction

Podocyte injury is now appreciated to be at the crux of many forms of proteinuric kidney diseases[1], identification of novel pathophysiological pathways and molecules in the podocytes is of priority in preventing glomerular disease progression and providing new opportunities for future treatment. During development, tight junctions (TJs) connect immature podocytes at an early stage and disappear along with the widening of the intercellular spaces and the appearance of slit diaphragm (SDs)[2,3]. Although mature podocytes lack TJs and form SDs between opposing foot processes, several claudins (CLDNs), the TJ-specific integral membrane protein, have been detected in podocytes of adult mouse kidneys, such as CLDN3 in nephrin knockout mice[4] and CLDN1 from animals with DN[5]. However, CLDN5 is the major CLDN expressed throughout the plasma membrane of mature podocytes under normal conditions[6]. Surprisingly, even 10 years after the discovery of CLDN5 in podocytes, little is known about the functional role of CLDN5 in glomerular physiology and disease development.

CLDN5 is unique among CLDN family members as its predominant expression in the endothelia and non-redundant function in the control of vascular permeability. CLDN5 deficient mice are born alive, but die within 10 h after birth without any morphological abnormalities[7]. In the current study, using podocyte specific Cldn5 knockout mice as a model, we report a previously unknown role of CLDN5 in the regulation of podocyte homeostasis. We reveal a mechanism whereby CLDN5 absence affects podocyte disease states through the transcriptional downregulation of WNT inhibitor factor-1 (WIF1), which leads to activation of WNT signaling pathway. By contrast, knockout Wif1 in podocytes results in the development of proteinuria and the typical ultrastructure change occurring in Cldn5 knockout mice. More importantly, targeted delivery of Wif1 to podocytes prevents the development of glomerular nephropathy in Cldn5

knockout diabetic mice, introducing WIF1 as a therapeutic target for mitigating podocyte injury. Because WIF1 is a secreted antagonist of the WNT pathway, we hypothesized that reduced podocyte secretion of WIF1 would result in activation of WNT signaling in renal tubule epithelial cells and lead to increased maladaptive repair of the kidney following injury. To test this hypothesis, we subjected these mice to tubular injury with unilateral ureteral obstruction (UUO). We found that the animals with podocyte deletion of Cldn5 or Wif1 gene had worse kidney fibrosis following UUO when compared with littermate controls with intact podocyte WIF1 expression. We also provided mechanistic insights into the regulation of Wif1 by CDLN5 by showing that CLDN5 affect the subcellular localization of the transcription factor ZO1 associated nucleic acid binding protein (ZONAB), which directly regulate Wif1 expression through interaction with its 3'-UTR.

Results

Generation and characterization of podocyte-specific Cldn5 knockout mice

Previous studies demonstrated CLDN5 is highly expressed in podocytes[6], suggesting that it might play important roles in maintaining glomerular health. To bypass the postnatal lethality of constitutive deletion and investigate the role of CLDN5 specifically in podocytes, we created $Cldn5^{loxP}$ mice, in which the Cldn5 mutated allele contains exon 1 flanked by loxP sites, in the C57BL/6J background (Fig. 1a). Next, we generated mice with podocyte-specific deletion of Cldn5 by intercrossing $Nphs2^{cre}$ and $Cldn5^{loxP/loxP}$ animals (Fig. 1b). Because Cre is known to have nonspecific effects that could influence podocytes[8], we studied 2 groups of mice: Nphs2-$Cre^{+/-}$/$Cldn5^{loxP/+}$ and Nphs2-$Cre^{+/-}$/$Cldn5^{loxP/loxP}$ mice, hereafter referred to as $Cldn5^{ctrl}$ and $Cldn5^{podKO}$ mice. Successful deletion of Cldn5 from $Cldn5^{podKO}$ mice was confirmed by quantitative PCR–based transcript analysis of isolated glomerulus (Fig. 1c). CLDN5 was colocalized with podocyte specific marker podocin (NPHS2) in $Cldn5^{ctrl}$ mice, consistent with a podocyte source (Fig. 1d). Immunofluorescence staining, as indicated by the lack of CLDN5 colocalization with NPHS2 in $Cldn5^{podKO}$ kidneys, but appropriate signal in the endothelial cells of arteriole, confirmed that the Nphs2-Cre–mediated Cldn5 deletion was largely confined to podocytes (Fig. 1d). Likewise, western blot analyses of CLDN5 expression showed a significant decrease in CLDN5 expression (approximately 77%) in glomerulus from $Cldn5^{podKO}$ mice (Fig. 1e), suggesting that CLDN5 expression in podocytes accounts for the majority of CLDN5 in normal glomerulus. The knockout mice didn't show compensated and increased expression of other TJ proteins CLDN1, CLDN3, or CLDN6 in podocytes (Supplemental Fig. 1).

We next investigated whether reduced CLDN5 expression in itself could cause proteinuria directly, using our engineered mice with a podocyte-specific targeted deletion of Cldn5. The age-matched $Cldn5^{ctrl}$ and $Cldn5^{podKO}$ mice were analyzed for the albuminuria abundance levels in spot urine samples at different time points. $Cldn5^{podKO}$ mice showed no albuminuria in early stages and began to appear at around 12 weeks (Fig. 1f). There was no significant difference in body weight, urine volume and urinary osmolality throughout the observation period from 3 to 48 weeks (data not shown). Blood urea nitrogen (BUN) levels

were within the normal values in both the groups (Fig. 1g). To investigate whether the appeared albuminuria was due to damage of the glomerular filtration barrier, we examined the kidney ultrastructure by transmission electron microscopy (TEM) in Cldn5^{podKO} and Cldn5^{ctrl} kidneys. TEM studies showed global thickening of the glomerular basement membrane (GBM) in Cldn5^{podKO} mice (Fig. 1h). GBM abnormalities were clear at 8 weeks of age and gradually aggravated by 24 weeks (Fig. 1h). In addition, podocyte foot processes appeared abnormal with broadening and effacement, which were notable in areas of severe GBM thickening (Fig. 1h). Control littermates developed mild GBM and foot processes changes after 24 weeks of age (Fig. 1h). Histological staining with periodic acid-Schiff staining (PAS) identified that Cldn5^{podKO} mice showed mesangial expansion and glomerular matrix accumulation at 24 weeks old compared with their littermate control mice (Fig. 1i). Quantitative PCR–based transcript analysis and immunofluorescence staining revealed that the expression of podocalyxin (PODXL) was reduced in Cldn5^{podKO} mice, which further confirmed podocyte damage (Supplemental Fig. 2). In summary, mice with podocyte-specific deficiency of CLDN5 showed early GBM alterations followed by later development of albuminuria.

Cldn5 deletion in podocytes accelerates DN progression

To determine whether CLDN5 has a role in diabetic kidney disease, we first studied the expression of CLDN5 in 2 mouse models of DN, the unilateral nephrectomy (UNX) combined with streptozotocin (STZ)-induced type I diabetic mice and DB/DB type 2 diabetic mice, by double immunostaining of CLDN5 and NPHS2. In both strains, we found that the expression of CLDN5 was decreased, which was accompanied by an attenuation in nephrin (NPHS1) and NPHS2 expression (Fig. 2a and 2b, Supplemental Fig. 3a and 3b). To determine whether the changes in CLDN5 expression also occur in human glomerular diseases, we queried the published transcriptomic data sets in kidney disease compiled in the Nephroseq database (nephroseq.org). CLDN5 mRNA expression was significantly reduced in the glomerulus of DN patients compared with those of healthy controls (Supplemental Fig. 3c). These findings suggest that loss of CLDN5 may play critical roles in the progression of DN. Then, to further investigate the effects of CLDN5 on DN development, STZ-induced DN mice with or without CLDN5 knockout were used. The Cldn5^{podKO} diabetic mice showed an increase in albuminuria as early 4 week after STZ injection, remaining elevated up to 12 weeks and reaching a difference of more than 4-fold compared with control diabetic mice of the same age (Fig. 2c). PAS staining revealed nodular glomerulosclerosis with increased amounts of extracellular matrix material in two groups of diabetic mice, which was exacerbated in Cldn5^{podKO} diabetic mice (Fig. 2d). TEM analysis demonstrated that GBM thickening and foot process effacement were induced, and these effects were significantly aggravated in Cldn5^{podKO} mice post to STZ treatment (Fig. 2e), which consistent with their more severe albuminuria. Podocyte injury was confirmed with increased expression of podocyte injury indicator desmin (Fig. 2f) and reduced expression of key podocyte markers, NPHS1, NPHS2, and PODXL (Supplemental Fig. 3d-i) in the Cldn5^{podKO} diabetic mice, as compared with the Cldn5^{ctrl} diabetic group. Masson Trichrome staining also showed a significant increase in interstitial fibrosis in the Cldn5^{podKO} diabetic mice (Fig. 2g). These results indicate the higher susceptibility to diabetic injury in the Cldn5^{podKO} mice.

Decreased Wif1 expression is observed in Cldn5 knockout glomerulus

To obtain insights into what might explain the phenotype of Cldn5 deletion in podocytes, we performed RNA-seq of glomerular lysates from $Cldn5^{ctrl}$ and $Cldn5^{podKO}$ mice. This unbiased analysis identified 280 downregulated genes and 102 upregulated genes (Fig. 3a). We found that, among the significantly altered genes by CLDN5 deletion, Wif1 reached remarkably high level (Fig. 3a). Data were validated by qRT-PCR (Fig. 3b) and immunofluorescence (Fig. 3c) performed on the kidney. Comparable results were obtained by qRT-PCR (Fig. 3d) and western blot analysis (Fig. 3e) on glomerulus isolated from mutant and wild-type littermates. WIF1 is a secreted WNT inhibitor, which exerts its inhibitory effect on WNT signaling by binding and inhibiting the activity of extracellular WNT ligands. This finding prompted us to speculate that CLDN5 depletion may lead to downregulation of WIF1 thereby activating WNT signaling. We found that WNT/β-catenin signaling was hyperactivated in $Cldn5^{podKO}$ podocytes based upon upregulated active nuclear β-catenin (CTNNB1) expression in $Cldn5^{podKO}$ podocytes compared to $Cldn5^{ctrl}$ podocytes (Fig. 3f). Notably, we found the same expression fingerprint of β-catenin target genes, including increased expression in CCND1 and CD44 (Fig. 3e, 3g-j). Previous studies in animals and humans have shown that CD44 is not expressed in healthy kidney, and activated parietal epithelial cells, but not podocytes, upregulate their *de novo* expression of CD44 during glomerular diseases[9,10]. In our study, although several of the variable CD44 isoforms were detected, mRNA levels of CD44v3 and CD44v5 appeared considerably higher expressed in the glomerulus from knockout mice than in those from control littermates (Fig. 3k). To determine whether dysregulation of WIF1 also occur in glomerulus with podocyte injury, we performed real-time PCR and immunostaining analysis. In comparison to control mouse glomerulus, WIF1 mRNA expression was significantly reduced in DN mice (Fig. 3l and 3m). WIF1 staining was significantly higher in the control while a dramatic loss of WIF1 staining was observed in these mice (data not shown). Collectively, these results indicate that the WNT pathway was activated by WIF1 inhibition in the mutant podocytes, resulting in the subsequent podocyte injury. These results identify CLDN5 as a potentially novel regulator of WNT/β-catenin signaling activity in podocytes.

Wif1 ablation mimics the phenotypes observed in Cldn5-deficient podocytes

To mimic the Wif1 downregulation observed in $Cldn5^{podKO}$ mice, we next constructed conditional knockout mice with podocyte-specific ablation of Wif1 by using the Cre-LoxP system. We generated $Wif1^{loxP}$ mice, in which the Wif1 mutated allele contains exon 3 flanked by loxP sites, in the C57BL/6J background (Supplemental Fig.4a). Next, we generated mice with podocyte-specific deletion of Wif1 by intercrossing $Nphs2^{cre}$ and $Wif1^{loxP/loxP}$ animals (Supplemental Fig. 4b). No residual Wif1-transcript or protein was detectable as determined by qRT-PCR, immunoblot, immunofluorescence in glomerular lysates or kidney sections in Nphs2-$Cre^{+/-}$/$Wif1^{loxP/loxP}$ (referred to as $Wif1^{podKO}$) mice (Fig. 4a-c), indicating WIF1 is expressed predominantly in podocytes in the kidney. Our data is in agreement with the single-cell RNA sequencing datasets of mouse kidney which indicated that Wif1 is expressed exclusively in podocytes (Supplemental Fig. 4c and 4d)[11,12]. To determine whether deletion of Wif1 in podocyte leads to activation of canonical WNT signaling, we studied the expression of several putative WNT/β-catenin

target genes in the glomerulus. We found CCND1 and CD44 were upregulated in Wif1^{podKO} mouse glomerulus (Supplemental Fig.4e and 4f). Wif1 KO mice had normal renal histology at 16 weeks of age, but TEM revealed thicker GBM which remains completely covered by the foot processes of the podocytes, but in areas with GBM thickenings foot process effacement was observed (Fig. 4d). Although genetic deletion of Wif1 resulted in the similar glomerular phenotype, the phenotypes observed in these mouse models were less severe than in the Cldn5^{podKO} mice. Consistent with this, podocyte-specific Wif1 mutant mice developed mild albuminuria at 16 weeks of age, 1.7-fold higher than control mice (Fig. 4e). The incomplete phenocopy of podocyte-specific Wif1 KO mice with Cldn5 KO mice led us to conclude that additional pathway maybe involved in the kidney pathogenesis associated with Cldn5 deletion.

AAV9-mediated WIF1 gain of function in podocytes ameliorates the progression of DN in Cldn5 KO mice

To further investigate the relevance of WIF1 to glomerular phenotype in Cldn5^{podKO} mice, we went on to test whether podocyte-specific WIF1 overexpression could rescue the phenotype of Cldn5^{podKO} mice. To overexpress WIF1 in podocytes, we used an AAV9 system with kidney in situ injection which has been proved to primarily transduce cells within the glomerulus of the kidney[13]. Podocyte-specific WIF1 delivery rescued the glomerular injury phenotype of diabetic Cldn5^{podKO} mice, including profound reduction of urine albumin-to-creatinine ratio (Fig. 4f), reduced foot process effacement, and decreased extracellular matrix deposition, as evidenced by PAS staining (Fig. 4g) and electron microscopy analysis (Fig. 4h). We also observed significantly less podocytes loss in WIF1-treatment group compared with the mutant mice treated with control AAV (podocyte number/glomerulus: AAV-WIF1 versus AAV-CTL: 11.583 ± 0.045 versus 10.167 ± 0.035, $P < 0.05$, n=10 mice/group) (Fig. 4i). Taken together, these results show a striking normalization of podocytes upon WIF1 administration in Cldn5^{podKO} diabetic mouse model, suggesting new avenues for the development of therapeutic strategies to ameliorate podocyopathy in DN.

Podocyte-specific loss of CLDN5 or WIF1 exacerbates interstitial fibrosis in UUO mouse model

Our data indicated that the phenotype changes in Cldn5^{podKO} podocytes aggravated interstitial fibrosis in DN mouse model (Fig. 2g). Because WIF1 is predominantly expressed in the podocytes, it could play a paracrine role on tubular epithelial cells through constant secretion into the preurine as a carrier. As WNT is an essential modulator of fibrosis development, we reasoned that local production of WIF1 by podocytes might affect WNT pathway tone in proximal tubules and participate in the progression of fibrosis following acute kidney injury. In spite of the fact that genetic deletion is limited to podocytes, both Wif1^{podKO} and Cldn5^{podKO} kidneys showed comparatively higher expression of the tubular damage markers KIM1, αSMA and collagen I compared with their littermates at 14 days of UUO (Fig. 5a and 5b). Kidney histological analysis using Masson's Trichrome staining showed that histological changes induced by UUO were markedly aggravated in CLDN5 or WIF1 deficient mice (Fig. 5c and 5d). Moreover, this effect was accompanied by up-regulated WNT downstream gene expression including CCND1 and CD44 (Fig. 5e and 5f). To demonstrate directly that podocyte secrete factors capable of silencing WNT signaling in proximal tubular cells, we assessed levels of the WNT target genes in cultured TKPTS

exposed to podocyte culture medium. We found that exposure of TKPTS to culture medium from $Cldn5^{podKO}$ podocytes resulted in the increased expression of WNT target genes including Mmp7, Tcf7, Cd44, Lef1, and Ccnd1 in TKPTS, compared with the culture medium from $Cldn5^{ctrl}$ podocytes which has higher concentration of WIF1 (Supplemental Fig. 5b-d). These data suggest that inadequate WIF1 secreted by podocytes in the Cldn5 and Wif1 knockout mouse permits exaggerated kidney damage and fibrosis during UUO via WNT-dependent actions in tubular epithelial cells. Thus, paracrine signals from podocytes that include WIF1 likely interact with proximal tubular cells and are essential to maintain its WNT pathway activity.

CLDN5 interacts with ZO1 and ZONAB in podocytes

The significant transcriptional downregulation of WIF1 by CLDN5 absence promoted us to identify the underlying molecular mechanisms linking them. On the basis of the information currently available, ZO1 form scaffolds to anchor TJ membrane proteins, and it also play very important roles in the control of gene expression via binding to and tuning the activity of transcription factor ZONAB[14,15]. To directly document the interaction between CLDN5 and ZO1/ZONAB complex, we performed coimmunoprecipitation (CoIP) in sparsely plated HEK293 cells transfected with four genes simultaneously. In HEK293 cells multiply transfected with CLDN5, ZO1, ZONAB variant 1, and ZONAB variant 2, anti-CLDN5 antibody precipitated ZO1 and ZONAB, and reciprocally, ZO1 co-immunoprecipitated with CLDN5 and ZONAB using the anti-ZO1 antibody, ZONAB co-immunoprecipitated with ZO1 and CLDN5 using the anti-ZONAB antibody (Fig. 6a). To test whether CLDN5 and ZO1/ZONAB are associated in native tissue, glomerular extracts were immunoprecipitated with anti-ZO1, anti-CLDN5 and anti-ZONAB, and precipitation of the three proteins was monitored by immunoblotting. We confirmed the endogenous interaction between CLDN5, ZO1, and ZONAB from glomerular extracts (Fig 6b). Together, these data reflect the existence of a complex containing CLDN5, ZO1, and ZONAB in the podocytes.

Podocytes CLDN5 deficiency increases ZONAB nuclear localization

We next asked whether Cldn5 knockout deregulates ZO1/ZONAB signaling in the podocytes. A marked reduction and more fragmented of ZO1 expression were observed in the Cldn5 KO mice compared with their wild-type littermates (Fig. 6c). Real-time quantitative PCR showed that the mRNA level of ZO1 was not significantly changed after Cldn5 deletion (data not shown), suggesting that the downregulation of ZO1 occurred at the protein level, possibly by higher levels of degradation. Confocal imaging showed membrane, cytoplasmic and weak nuclear ZONAB labeling in $Cldn5^{ctrl}$ mouse glomerulus and a distinct colocalization of ZONAB with WT1 in $Cldn5^{podKO}$ mice (Fig. 6d), which indicated CLDN5 deletion in podocytes increased ZONAB nuclear localization. Subcellular fractionation of the isolated glomerulus, followed by western blot analyses, indicated that CLDN5 deletion and ZO1 reduction in podocytes promoted ZONAB to undergo nuclear translocation (Fig. 6e). We then determined whether the effects of CLDN5 deletion on Wif1 expression could be rescued by re-introduction of ZO1. Co-transfection of CLDN5-defiencient primary podocytes with Zo1 and Cldn5, but not transfection with Zo1 alone, showed

an increase in Wif1 expression (Fig. 6f), indicating a functional interaction between CLDN5 and ZO1 in the regulation of Wif1. Taken together, our data so far indicate that CLDN5 forms a complex with ZO1 and ZONAB in normal podocytes under physiologic conditions, and this complex is required to sustain ZONAB's subcellular localization and adequate levels of WIF1 to maintain normal WNT signaling activity.

ZONAB regulates Wif1 expression through its 3'-UTR

We next analyzed the molecular mechanism by which ZONAB reduced the expression of Wif1 mRNA. Transcript levels can be altered by changes in transcription, RNA processing, mRNA stability, or a combination thereof, and ZONAB has been suggested to have roles in all these processes. To address these possibilities, we first evaluated whether ZONAB plays a transcriptional role on Wif1 promoter, we performed reporter gene assays by transiently transfecting into primary podocytes and MDCK cells a plasmid construct containing the firefly luciferase gene driven by the Wif1 promoter fragments together with Zonab or its vector control. This analysis showed little to no effect on Wif1 mRNA (Fig. 6g and 6h), suggesting that Wif1 mRNA abundance regulation by ZONAB is not mediated by its 5'-promoter. Next, we set out to understand if ZONAB targets Wif1 3'-UTR, we generated the reporter constructs that had the entire mouse Wif1 3'-UTR sequence cloned downstream of the renilla luciferase gene. The reporter was transfected with Zonab to primary podocytes and MDCK cells. When both cells were co-transfected with a ZONAB expression vector (pCMV6-Zonab-V1 or pCMV6-Zonab-V2), the luciferase activities were decreased (Fig 6i and 6j), thus providing evidence that ZONAB acts as a repressor factor of Wif1 expression by its 3'-UTR. To verify that ZONAB is capable of inhibiting the endogenous WIF1 in native podocytes, we knocked down Zonab with specific siRNA and analyzed the expression level of Wif1 via real-time RT-PCR. Following knockdown of Zonab mRNA, qRT-PCR revealed significantly elevated levels of Wif1 transcript in $Cldn5^{podKO}$ podocytes compared to cells treated with control siRNA (Fig. 6k). Taken as a whole, our results establish that transcriptional regulation of WIF1 by ZONAB at least in part is brought about via repression of the Wif1 3'-UTR.

Discussion

Firstly, we showed that mice with podocyte-specific deletion of Cldn5 manifested albuminuria but not glomerulosclerosis, as least within our observation period. When we looked at kidney under the electron microscope, TEM revealed the presence of thickening of the GBM and mild foot process effacement. Furthermore, we observed a significant reduction in CLDN5 expression in two DN mouse models. It has been shown the TJs scaffold protein ZO1 is likewise reduced in the same conditions[16], further study is required to determine whether reduced expression of ZO1 is a consequence of diminished podocyte CLDN5 in these diseases, or *vice versa*. Crucially, in two DN models, animals with a podocyte-specific deletion of CLDN5 manifest a more severe nephropathy, including more proteinuria, and evidence of more podocyte injury, but interestingly also more severe interstitial fibrosis. These results indicate that CLDN5 is a critical injury response gene in podocytes with a strong linkage to kidney injury.

In an attempt to determine the underlying mechanism, we found that Cldn5 deletion in podocytes repressed expression of Wif1. WIF1 is a secreted protein that functions as a paracrine inhibitor of the WNT signaling pathway by binding, and inhibiting the activity of extracellular WNT ligands[17]. Aberrant activation of WNT/β-catenin signaling plays a central role in the pathogenesis of a wide variety of kidney disease[18,19]. A highly prevalent nuclear β-catenin expression and an overactivated WNT/β-catenin signaling in podocytes of patients and mouse models of diabetic kidney disease have fueled the concept that hyperactivated WNT-signaling promotes glomerular disease progression[20]. The result of present study showed that the deletion of CLDN5 leads to activated WNT/β-catenin signaling in podocytes via downregulation of Wif1, resulting in similar base-line phenotype to the podocyte-specific stabilized Ctnnb1 expression mice[21]. More importantly, targeted delivery of Wif1 obviated the development of DN in Cldn5 knockout mice as demonstrated by the preservation of podocyte foot process and reduced extracellular matrix deposition in the glomerulus. Ultrastructural examination of podocyte-specific conditional Wif1-knockout kidneys showed irregular thickening of the GBM with occasional regions of foot processes effacement, mimicking the phenotypes of Cldn5-deficient podocytes. Therefore, our results establish that CLDN5 is a novel regulator of WNT/β-catenin signaling activity in podocytes. Our current findings are well in accordance with other group's earlier findings. Genetic manipulation of CLDN18 in stomach cause subtle changes in β-catenin localization and upregulation of downstream effectors CD44, EFNB1 and B2, and EPHB2[22]. CLDN3 loss induces WNT/β-catenin activation and help promote colon cancer[23]. Thus, we describe a novel role of CLDN5 in its capacity to avert WNT-signaling hyperactivation in podocytes via transcriptional regulation of WIF1 expression.

In addition, we identify WIF1 as a factor secreted by podocytes that may also contribute to tubular dysfunction in chronic kidney disease. The progression of primary glomerular disease to induce tubulointerstitial lesions is well established, the mechanisms by which glomerular injury extends to proximal tubules are still under investigation. Although filtered albumin is considered central to the extension of glomerular injury to proximal tubules[24], whether paracrine mechanisms are active in the progression of tubulointerstitial abnormalities require more investigation. A recent study proved podocyte-derived microparticles induce pro-fibrotic responses in proximal tubular cells[25], indicating cross-talk between podocytes and the tubular epithelium through paracrine signaling play roles in the development of tubulointerstitial fibrosis in chronic kidney disease. Blockade of WIF1 secretion by genetic deletion of Cldn5 or Wif1 in podocytes markedly enhanced renal fibrosis after UUO. This effect was associated with increased WNT downstream genes expression. *In vitro,* exposure of TKPTS to culture medium from Cldn5-deficient podocytes result in the increased expression of WNT target genes, compared with the culture medium from wild-type podocytes which has higher concentration of WIF1. Such podocyte-derived WIF1 causes deleterious tubular injury changes, however, it remains unclear whether it inhibit one specific WNT, or a group of WNTs, that contribute to fibrosis development[26]. Collectively, these data add strong support for a potentially novel mechanism to account for how glomerular injury triggers tubular damage during chronic kidney disease progression.

CLDN5 interacts with a cytoplasmic plaque that consists of adaptor proteins, such as ZO1, that recruits signaling molecules and interact with the actin cytoskeleton. These components recruit different types of signaling proteins that regulate junctional functions as well as cell behavior. Some of the preliminary evidence that ZO proteins participated in the control of gene expression was the observation that the transcription factor ZONAB was expressed in the nucleus and also co-localized with ZO1 to form a complex[14,27,28]. We show here that the interaction of ZO1 with CLDN5 may be important for the stabilization of ZO1 in podocytes via anchoring ZO1 to the plasma membrane to inhibit nuclear accumulation of ZONAB. ZONAB localization in podocytes is affected by Cldn5 knockout along with biochemical interactions between CLDN5, ZO1, and ZONAB. And altered ZO1 distribution in Cldn5 knockout mice provide increasing evidence for functional interactions between these proteins. Loss of CLDN5 likely disrupts this membrane protein complex and induces the translocation of ZONAB into the nucleus, leading to downregulation of WIF1. Even though ZO1 has been identified as an important component of the SD complex and podocyte-specific deletion of ZO1 gene impaired SDs formation[29], we did not observe *bona fide* SDs morphological defect in our animals despite a significant reduction in ZO1 expression. We do not currently know why such a difference exists, one possibility is that the signal strengths generated by the CLDN5 deficiency are different from ZO1 knockout, leading to their different outcome.

ZONAB is a Y-box transcription factor also known as YB-3, MSY4 (in mice), and DNA binding protein A or cold shock domain protein A (in human)[30]. As a nucleic-acid-binding protein that directly regulates gene expression by different mechanisms, ZONAB has been reported to be involved in transcriptional activation and repression, as well as in posttranscriptional mechanisms of gene expression regulation, including mRNA packaging, transport, localization and stability[14,27,31]. Here, we show that the transcriptional level of Wif1 mRNA is directly regulated by ZONAB in the podocytes, whereas the promoter activity of Wif1 is not affected. Although ZONAB has been proved to act as a positive regulator of mRNA abundance by binding to 3'-UTRs, we show here the transcriptional regulation of WIF1 by ZONAB is brought about via 3'-UTR-mediated repression. Our observations are consistent with a recent study demonstrating that both reduced and increased transcripts were observed upon loss of ZONAB via integrated proteomic and transcriptomic analysis from cells depleted of ZONAB[32]. The 3'-UTRs play important roles in controlling mRNA stability, localization, translation and degradation, it would be of immense interest to explore the mechanism by which ZONAB lowers Wif1 expression.

In conclusion, the present study reveals a previously undescribed function and an important regulatory role for TJ protein CLDN5 in restricting WNT activity in the kidney (Supplemental Fig. 6). The paradigm of CLDN5 restricting WNT signaling can therefore be extended to other sites of CLDN5 expression. Interestingly, CLDN5 is regulated by WNT signaling[33], suggesting that it might participate in a negative feedback loop to limit WNT-initiated signals. Our experiments also provide a proof of principle that CLDN5 and WIF1 might be developed into therapeutic modalities for the treatment of kidney diseases affecting millions of people worldwide.

Materials And Methods

Antibodies, plasmids, and cell lines

The antibodies used in this study are summarized in Supplemental Table 1. The full-length cDNA of mouse Zo1 (NM_009386) was synthesized and cloned into pLVX vector by Sango Biotechnology (China). The expression plasmids containing mouse Cldn5 (pCMV6-Cldn5, NM_013805,), Zonab transcript variant 1 (pCMV6-Zonab-V1, NM_139117), and Zonab transcript variant 2 (pCMV6-Zonab-V2, NM_011733) genes were purchased from Origene Technologies (USA). MDCK II, human HEK293 cells, 3T3-L1, and mouse proximal tubule cells (TKPTS) were obtained from ATCC (USA) and cultured according to the distributor's recommendations.

Animals

All animals were maintained in specific pathogen-free facilities. The 12-week-old male DB/M and DB/DB were obtained from Cavens Biogle (China). C57BL/6J (B6) mice were obtained from Vital River Laboratory (China).

For the generation of $Cldn5^{loxP/loxP}$ mice, targeting vector was constructed by inserting one SDA (self-deletion anchor)-flanked neomycin cassette and two loxP sites flanking the first exon of Cldn5 and then electroporating into embryonic stem cells from C57BL/6J mice (conducted by Cyagen Biosciences Inc, China). With one subsequent cross with B6 animals, the Neo transgene was removed and the obtained $Cldn5^{loxP/+}$ mice were then intercrossed in order to generate the $Cldn5^{loxP/loxP}$ mice. Same strategy was used to generate the $Wif1^{loxP/loxP}$ mice with exon 3 selected as conditional knockout region.

$Cldn5^{loxP/loxP}$ mice or $Wif1^{loxP/loxP}$ mice were crossed with Nphs2-Cre mice (Jackson Laboratory, 008205) to generate podocyte-specific Cldn5 knockout mice Nphs2-$Cre^{+/-}$/$Cldn5^{loxP/loxP}$ ($Cldn5^{podKO}$) or podocyte-specific Wlf1 knockout mice Nphs2-$Cre^{+/-}$/$Wif1^{loxP/loxP}$ ($Wif1^{podKO}$), respectively. Heterozygous with Nphs2-Cre positive litter mates served as controls.

R26-stop-EYFP reporter mice harbor a conditional Enhanced Yellow Fluorescent Protein (EYFP) allele that requires Cre mediated recombination for expression. To facilitate the isolation of primary podocytes by fluorescence-activated cell sorting (FACS), we crossed R26-stop-EYFP mutant mice (Jackson Laboratory, 006148) with $Cldn5^{podKO}$ mice to get podocyte-specific Cldn5 knockout reporter mice (Nphs2-$Cre^{+/-}$/$Cldn5^{loxP/loxP}$/EYFP-$stop^{loxP/loxP}$) and control reporter mice (Nphs2-$Cre^{+/-}$/$Cldn5^{loxP/-}$/EYFP-$stop^{loxP/loxP}$) (Supplemental Fig. 5a).

STZ-induced diabetic nephropathy (DN)

Unilateral nephrectomy (UNX) combined with streptozotocin (STZ) were used to accelerate the development of DN. Briefly, after a 1-week recovery period from UNX, STZ was injected into 5-7 weeks old fasting $Cldn5^{ctrl}$ and $Cldn5^{podKO}$ mice (intraperitoneal injection of 50 mg/kg body weight) for 5 days. Spot

samples of urine were collected every 4 weeks. Urinary albumin excretion rates were analyzed 4, 8, and 12 weeks after the last injection of STZ. Kidneys were harvested and processed for histological and ultrastructural analyses, glomerulus were collected for qRT-PCR and western blot analysis after the 12-week follow-up.

In vivo administration of recombinant AAV

rAAV9 is the most efficient rAAV serotype for kidney gene delivery[34]. To overcome the non-specificity of rAAV9, we utilized the rAAV9 vector containing the Nphs1 promoter to drive expression of WIF1 in podocytes. 4-6 weeks $Cldn5^{podKO}$ mice were performed with UNX and injected with STZ as described above. After 4 weeks of STZ injection, mice received in situ renal injection with 1×10^{12} genomic particles of rAAV9-NPHS1-GFP (AAV-CTL) or rAAV9-NPHS1-WIF1 (AAV-Wif1) (prepared by Hanbio Biotechnology Inc, China) at five independent points. Spot samples of urine were collected every 4 weeks. All mice were sacrificed to harvest kidneys 8 weeks after transduction.

Unilateral ureteral obstruction (UUO)

8- to 10-week-old male mice were anesthetized and the left kidney exposed by the retroperitoneal approach. The ureter was ligated with 4-0 silk suture at 2 points, close to the renal pelvis. Kidneys were harvested for analysis 14 days after UUO.

Urine and serum analyses

Urinary albumin and creatinine were measured using mouse albumin–specific ELISA (Bethyl Laboratories, USA) and Quantichrome Creatinine Assay Kit (Nanjing Jiancheng, China). Proteinuria was expressed as μg albumin/mg creatinine. Blood glucose was measured using Yuwell Blood Glucose Meter (China). Plasma BUN was analyzed by

Histologic analysis

Paraffin-embedded mouse kidney sections (5 μm thickness) were prepared by a routine procedure. Sections were stained with periodic acid-Schiff (PAS) and Masson's Trichrome. Transmission electron microscopy (TEM) was performed on glutaraldehyde-fixed, epoxy-embedded kidney samples and stained with uranyl acetate and lead citrate.

Immunofluorescence staining

For immunofluorescence of kidney tissue, 8-μm frozen sections were fixed in ice-cold methanol or acetone. For immunofluorescence of cultured cells, primary podocytes on collagen I coated coverslips were fixed with 4% paraformaldehyde. Then incubated with the appropriate primary antibodies after blocking with 10% FBS in PBS, developed using FITC and/or rhodamine (TRITC) conjugated secondary antibodies (Millipore), and mounted with ProLong™ Gold Antifade Mountant.

RNA-sequencing (RNA-seq)

Total RNA was extracted using Trizol reagent (Invitrogen, 15596018) from glomerulus of $Cldn5^{ctrl}$ and $Cldn5^{podKO}$ mice at 4 weeks old. RNA-seq was performed on an Illumina Novaseq platform by Annoroad Genome (China). Paired-end clean reads were aligned to the mouse reference genome (Ensemble_GRCm38.90) with TopHat (version 2.0.12), and the aligned reads were used to quantify mRNA expression by using HTSeq-count (version 0.6.1). Differential expression analysis of two groups was performed using the DESeq2 R package (1.16.1). The resulting P-values were adjusted using the Benjamini and Hochberg's approach for controlling the false discovery rate. Genes with an adjusted P-value <0.05 found by DESeq2 were assigned as differentially expressed.

Primary podocytes isolation and treatment

Glomerulus were isolated from the $Cldn5^{ctrl}$ and $Cldn5^{podKO}$ mice expressing a GFP-reporter, by using Dynabeads M-450 Tosylactivated (#14013 Invitrogen) perfusion. The glomerulus were then further digested enzymatically (Multi Tissue Dissociation Kits, Miltenyi) and dissociated into a single-cell suspension by using the gentleMACS™ Dissociators, and FACS was used to isolate the GFP positive podocytes. For podocytes culture, RPMI 1640 supplemented with 10% fetal calf serum and 3T3-L1 medium were mixed in a 1:1 ratio as described[35]. The expression plasmid containing mouse Zo1 cDNA (pLVX-Zo1) was transfected alone or together with Cldn5 (pCMV6-Cldn5) into the Cldn5 deficient podocytes using lipofectamine 2000 (Invitrogen). For Zonab siRNA treatment, a pool of three target-specific 21 nt siRNA duplexes (Sango Biotechnology, China) were designed against the coding region of mouse Zonab gene (NM_139117, NM_011733). A scrambled siRNA duplex (Sango Biotechnology, China) was used as negative control. Either Zonab siRNA or scrambled siRNA was transfected to primary podocytes in 12-well culture dishes with lipofectamine 2000 for 24 h. RNA was subsequently extracted, and real-time qPCR was performed.

TKPTS cells experiment

In conditioned medium experiments, FACS-sorted WT or Cldn5 KO primary podocytes were cultured for 24 h. Supernatants were collected and cell debris was removed by centrifugation (2000 x g, 5 min.). TKPTS cells were stimulated with 50% podocyte supernatants, added to their usual culture medium for 12 h (Supplemental Fig. 5b). RNA was subsequently extracted, and real-time qPCR was performed.

RNA extraction and quantitative real time PCR

Total RNA was extracted from isolated glomerulus or cultured cells using Trizol (Ambion, USA). RNA was reverse transcribed by using a reverse transcription system kit according to the instructions of the manufacturer (Takara, Japan) followed by quantitative real time PCR (qRT-PCR) amplification using SYBR Green PCR Master Mix (ABI, USA) and the Thermo Fisher QuantStudio3 system. The Supplemental Table 2 contains the primer sequences used in this study. The expression levels of each mRNA were

calculated after normalizing to those of β-actin. Results were expressed as $2^{-\Delta Ct}$ values with $\Delta CT=Ct_{gene}-Ct_{\beta\text{-actin}}$.

Western blot analysis

Total protein extracts were obtained by lysing isolated glomerulus in 1× Laemmli buffer (50 mM Tris-Cl pH 7.5, 2% SDS, 10% glycerol, 5% β-mercaptoethanol, 0.01% bromophenol blue). Cellular fractions (membrane, cytoskeleton, cytosolic, and nuclear) obtained from glomerulus were extracted using the Chemicon Compartmental Protein Extraction Kit according to the manufacturer's instructions (Millipore). Protein expression was detected by SDS/PAGE under reducing conditions, and immunoblotting was performed with anti-CLDN5, anti-NPHS1, anti-WIF1, anti–CCND1, anti-CD44, and anti-tubulin antibodies. HRP-conjugated secondary antibodies (Thermo Fisher) followed by ECL (Thermo Fisher) incubation allowed protein band detection.

Luciferase reporter assay

The mouse Wif1 gene promoters (2 kb, 1 kb, and 0.5 kb before start codon of the Wif1 open reading frame, synthesized by Shanghai Sango Biotechnology) were cloned into pGL3-Basic luciferase reporter vector (Promega) with NheI and HindIII sites. The pGL3 reporter, the pGL4.74 Renilla luciferase control vector (Promega), and pCMV6-Zonab vector were cotransfected to MDCK cells and primary podocytes in 96-well culture dishes using lipofectamine-2000. The 771 bp 3'-UTR of mouse Wif1 gene (synthesized by Shanghai Sango Biotechnology) was inserted into the psiCHECK-2 (Clontech) downstream of the luciferase gene using XhoI/NotI. The psiCHECK-2-Wif1: 3'-UTR and pCMV6-Zonab vector were co-transfected to MDCK cells and primary podocytes in 96-well culture dishes using lipofectamine 2000. Twenty-four hours after transfection, firefly and renilla luciferase activities were measured with a chemiluminescence reporter assay system—Dual Glo (Promega) in Fluostar Omega (BMG).

Co-Immunoprecipitation (Co-IP)

Isolated glomerulus or HEK293 cells expressing CLDN5 with ZO1 and ZONAB were lysed in 50mM Tris (pH 8.0) by 25–30 repeated passages through a 25-gauge needle, followed by centrifugation at 5000 g. The membranes of lysis were extracted using CSK buffer (150 mM NaCl; 1% Triton X-100; 50 mM Tris, pH 8.0; and protease inhibitors). The membrane extract was precleared by incubation with protein A/G-sepharose (Sigma-Aldrich) prior to Co-IP. The precleared membrane extract was incubated for 16 h at 4 °C with anti-CLDN5, anti-ZO1, anti-ZONAB, and anti-mouse IgG (as negative control) antibodies. Antibody-bound material was pelleted with protein A/G-sepharose, washed three times with CSK buffer, and detected by immunoblotting.

Data availability

The raw RNA-seq data were deposited in NCBI sequence read archive (SRA) database, with the accession number PRJNA700678.

Statistical analyses

The significance of differences between groups was tested by Prism 6.07 (GraphPad Software Inc.). Statistical analysis was performed using the unpaired t test to determine differences between two groups and ANOVA to compare data among groups. P-values less than 0.05 were interpreted as statistically significant. All data are presented as mean ± SEM and other details such as the number of replicates and the level of significance is mentioned in figure legends and supplementary information.

Declarations

Study approval

All animal studies were approved by the Animal Ethics Committee of Binzhou Medical University.

Acknowledgments

We are grateful to George Jarad (Washington University in St. Louis) for helpful suggestions on the study. We thank Min Zhao and Ping Li for animal husbandry. We thank the Medicine and Pharmacy Research Center of Binzhou Medical University for assistance on electron microscopy imaging and FACS sorting. The work is funded by National Natural Science Foundation of China (81670620, 81870485, and 81971281), Taishan Scholars Program of Shandong Province (ts20190953), Natural Science Foundation of Shandong Province (ZR2020QH066), and Binzhou Medical University Independent Research Program.

Author contributions

J.Y., H.L. and H.S. performed animal characterization and *in vitro* studies. H.G. analyzed RNA-sequencing data. J.L. performed histologic analysis. X.M. and N.L. performed mice genotyping. X.W. and X.W. performed unilateral ureteral obstruction surgery. Y.G. designed and supervised the study, analyzed the data, and wrote the manuscript.

Competing Interests statement

The authors declare no competing financial interests.

References

1. Assady, S., Benzing, T., Kretzler, M. & Skorecki, K.L. Glomerular podocytes in kidney health and disease. *Lancet* **393**, 856-858 (2019).
2. Lehtonen, S.*, et al.* Cell junction-associated proteins IQGAP1, MAGI-2, CASK, spectrins, and alpha-actinin are components of the nephrin multiprotein complex. *Proceedings of the National Academy of Sciences of the United States of America* **102**, 9814-9819 (2005).
3. Quaggin, S.E. & Kreidberg, J.A. Development of the renal glomerulus: good neighbors and good fences. *Development* **135**, 609-620 (2008).

4. Done, S.C.*, et al.* Nephrin is involved in podocyte maturation but not survival during glomerular development. *Kidney international* **73**, 697-704 (2008).
5. Hasegawa, K.*, et al.* Renal tubular Sirt1 attenuates diabetic albuminuria by epigenetically suppressing Claudin-1 overexpression in podocytes. *Nature medicine* **19**, 1496-1504 (2013).
6. Koda, R.*, et al.* Novel expression of claudin-5 in glomerular podocytes. *Cell and tissue research* **343**, 637-648 (2011).
7. Nitta, T.*, et al.* Size-selective loosening of the blood-brain barrier in claudin-5-deficient mice. *The Journal of cell biology* **161**, 653-660 (2003).
8. Balkawade, R.S.*, et al.* Podocyte-specific expression of Cre recombinase promotes glomerular basement membrane thickening. *American journal of physiology. Renal physiology* **316**, F1026-F1040 (2019).
9. Chan, G.C.*, et al.* Differential expression of parietal epithelial cell and podocyte extracellular matrix proteins in focal segmental glomerulosclerosis and diabetic nephropathy. *American journal of physiology. Renal physiology* **317**, F1680-F1694 (2019).
10. Djudjaj, S.*, et al.* Macrophage Migration Inhibitory Factor Mediates Proliferative GN via CD74. *Journal of the American Society of Nephrology : JASN* **27**, 1650-1664 (2016).
11. Park, J.*, et al.* Single-cell transcriptomics of the mouse kidney reveals potential cellular targets of kidney disease. *Science* **360**, 758-763 (2018).
12. Wu, H., Kirita, Y., Donnelly, E.L. & Humphreys, B.D. Advantages of Single-Nucleus over Single-Cell RNA Sequencing of Adult Kidney: Rare Cell Types and Novel Cell States Revealed in Fibrosis. *Journal of the American Society of Nephrology : JASN* **30**, 23-32 (2019).
13. Picconi, J.L.*, et al.* Kidney-specific expression of GFP by in-utero delivery of pseudotyped adeno-associated virus 9. *Molecular therapy. Methods & clinical development* **1**, 14014 (2014).
14. Balda, M.S. & Matter, K. The tight junction protein ZO-1 and an interacting transcription factor regulate ErbB-2 expression. *The EMBO journal* **19**, 2024-2033 (2000).
15. Pozzi, A. & Zent, R. ZO-1 and ZONAB interact to regulate proximal tubular cell differentiation. *Journal of the American Society of Nephrology : JASN* **21**, 388-390 (2010).
16. Rincon-Choles, H.*, et al.* ZO-1 expression and phosphorylation in diabetic nephropathy. *Diabetes* **55**, 894-900 (2006).
17. Hsieh, J.C.*, et al.* A new secreted protein that binds to Wnt proteins and inhibits their activities. *Nature* **398**, 431-436 (1999).
18. Lee, E.J.*, et al.* TAZ/Wnt-beta-catenin/c-MYC axis regulates cystogenesis in polycystic kidney disease. *Proceedings of the National Academy of Sciences of the United States of America* **117**, 29001-29012 (2020).
19. Shkreli, M.*, et al.* Reversible cell-cycle entry in adult kidney podocytes through regulated control of telomerase and Wnt signaling. *Nature medicine* **18**, 111-119 (2011).

20. Dai, C.*, et al.* Wnt/beta-catenin signaling promotes podocyte dysfunction and albuminuria. *Journal of the American Society of Nephrology : JASN* **20**, 1997-2008 (2009).
21. Kato, H.*, et al.* Wnt/beta-catenin pathway in podocytes integrates cell adhesion, differentiation, and survival. *The Journal of biological chemistry* **286**, 26003-26015 (2011).
22. Hagen, S.J.*, et al.* Loss of Tight Junction Protein Claudin 18 Promotes Progressive Neoplasia Development in Mouse Stomach. *Gastroenterology* **155**, 1852-1867 (2018).
23. Ahmad, R.*, et al.* Loss of claudin-3 expression induces IL6/gp130/Stat3 signaling to promote colon cancer malignancy by hyperactivating Wnt/beta-catenin signaling. *Oncogene* **36**, 6592-6604 (2017).
24. Jarad, G., Knutsen, R.H., Mecham, R.P. & Miner, J.H. Albumin contributes to kidney disease progression in Alport syndrome. *American journal of physiology. Renal physiology* **311**, F120-130 (2016).
25. Munkonda, M.N.*, et al.* Podocyte-derived microparticles promote proximal tubule fibrotic signaling via p38 MAPK and CD36. *Journal of extracellular vesicles* **7**, 1432206 (2018).
26. Edeling, M., Ragi, G., Huang, S., Pavenstadt, H. & Susztak, K. Developmental signalling pathways in renal fibrosis: the roles of Notch, Wnt and Hedgehog. *Nature reviews. Nephrology* **12**, 426-439 (2016).
27. Nie, M., Balda, M.S. & Matter, K. Stress- and Rho-activated ZO-1-associated nucleic acid binding protein binding to p21 mRNA mediates stabilization, translation, and cell survival. *Proceedings of the National Academy of Sciences of the United States of America* **109**, 10897-10902 (2012).
28. Lima, W.R.*, et al.* ZONAB promotes proliferation and represses differentiation of proximal tubule epithelial cells. *Journal of the American Society of Nephrology : JASN* **21**, 478-488 (2010).
29. Itoh, M.*, et al.* The structural and functional organization of the podocyte filtration slits is regulated by Tjp1/ZO-1. *PloS one* **9**, e106621 (2014).
30. Arakawa, Y.*, et al.* Transcription of dbpA, a Y box binding protein, is positively regulated by E2F1: implications in hepatocarcinogenesis. *Biochemical and biophysical research communications* **322**, 297-302 (2004).
31. Sourisseau, T.*, et al.* Regulation of PCNA and cyclin D1 expression and epithelial morphogenesis by the ZO-1-regulated transcription factor ZONAB/DbpA. *Molecular and cellular biology* **26**, 2387-2398 (2006).
32. Cooke, A.*, et al.* The RNA-Binding Protein YBX3 Controls Amino Acid Levels by Regulating SLC mRNA Abundance. *Cell reports* **27**, 3097-3106 e3095 (2019).
33. Wang, Y.*, et al.* Norrin/Frizzled4 signaling in retinal vascular development and blood brain barrier plasticity. *Cell* **151**, 1332-1344 (2012).
34. Rocca, C.J., Ur, S.N., Harrison, F. & Cherqui, S. rAAV9 combined with renal vein injection is optimal for kidney-targeted gene delivery: conclusion of a comparative study. *Gene therapy* **21**, 618-628 (2014).
35. Shankland, S.J., Pippin, J.W., Reiser, J. & Mundel, P. Podocytes in culture: past, present, and future. *Kidney international* **72**, 26-36 (2007).

Figures

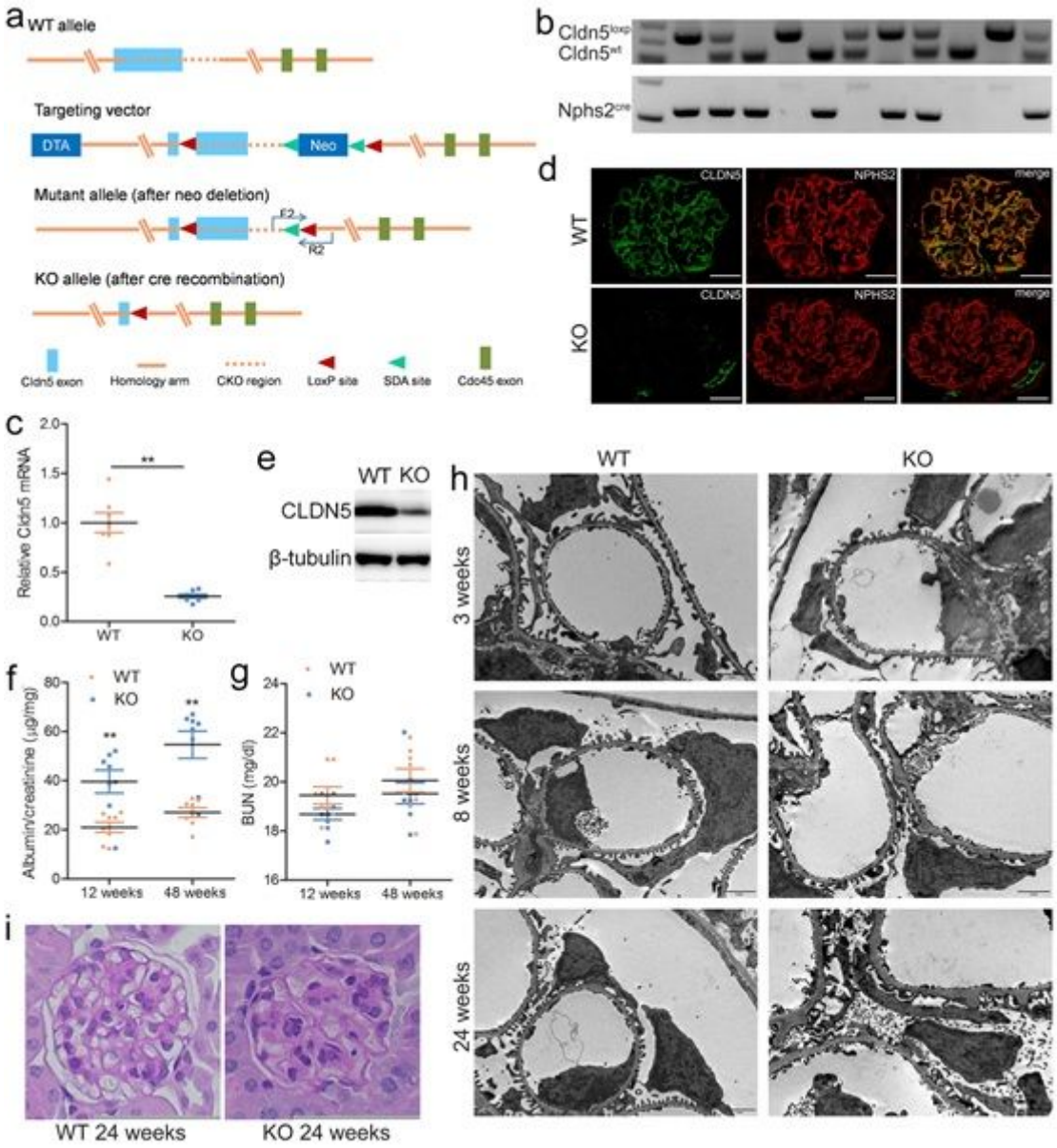

Figure 1

Generation and characterization of podocyte specific Cldn5 knockout mice. (a) Gene targeting strategy. The diagram showing the wild-type Cldn5 locus, the targeting construct, the mutant allele after neo deletion, and the knockout (KO) allele after Cre recombination. In the targeting vector, the neo cassette was flanked by SDA (self-deletion anchor) sites, and exon 1 of Cldn5 was flanked by loxP sites. The first loxP site was placed upstream of the ATG start codon with 8 bp. Diphtheria toxin A (DTA) was used for negative selection. (b) PCR verification of offspring tails, demonstrating WT (215 bp), heterozygous (215 bp and 328 bp), and homozygous (328 bp) alleles. The primer F2 is located on cKO (conditional knock out) region. The primer R2 is located downstream of the second loxP site. The Nphs2 Cre recombinase transgene was identified as a 200 bp PCR product. (c) qRT-PCR analysis in isolated glomerulus of WT and Cldn5 KO mice shows 75% reduction of Cldn5 mRNA in the KO mouse (n = 6, **P < 0.01). (d) CLDN5

(green) and NPHS2 (red) immunostaining of kidney sections from WT and Cldn5 KO mice. Scale bars, 20 μm. (e) Western blot analysis of isolated glomerulus confirm deletion of CLDN5 protein in the KO mouse. (f) Cldn5 KO mice display significant increase in albuminuria as determined by ELISA at 12 and 48 weeks of age (n = 8, **P < 0.01). The y axis shows the ratio of albumin to creatinine in spot urine compared to the control group. (g) Graph of plasma BUN levels at 12 and 48 weeks of age in KO mice compared to control littermates (n = 8). (h) TEM in WT and Cldn5 KO mice at 3, 8 and 24 weeks of age. At 24 weeks (lowest panel), the GBM in KO mice show thick and irregular basement membrane, whereas foot processes remain partially preserved. Scale bars, 5 μm. (i) PAS-stained images of kidney cortex from WT and Cldn5 KO mice showing thickening of GBM, mesangial expansion and glomerular matrix accumulation in KO mice at 24 weeks. Scale bars, 100 μm.

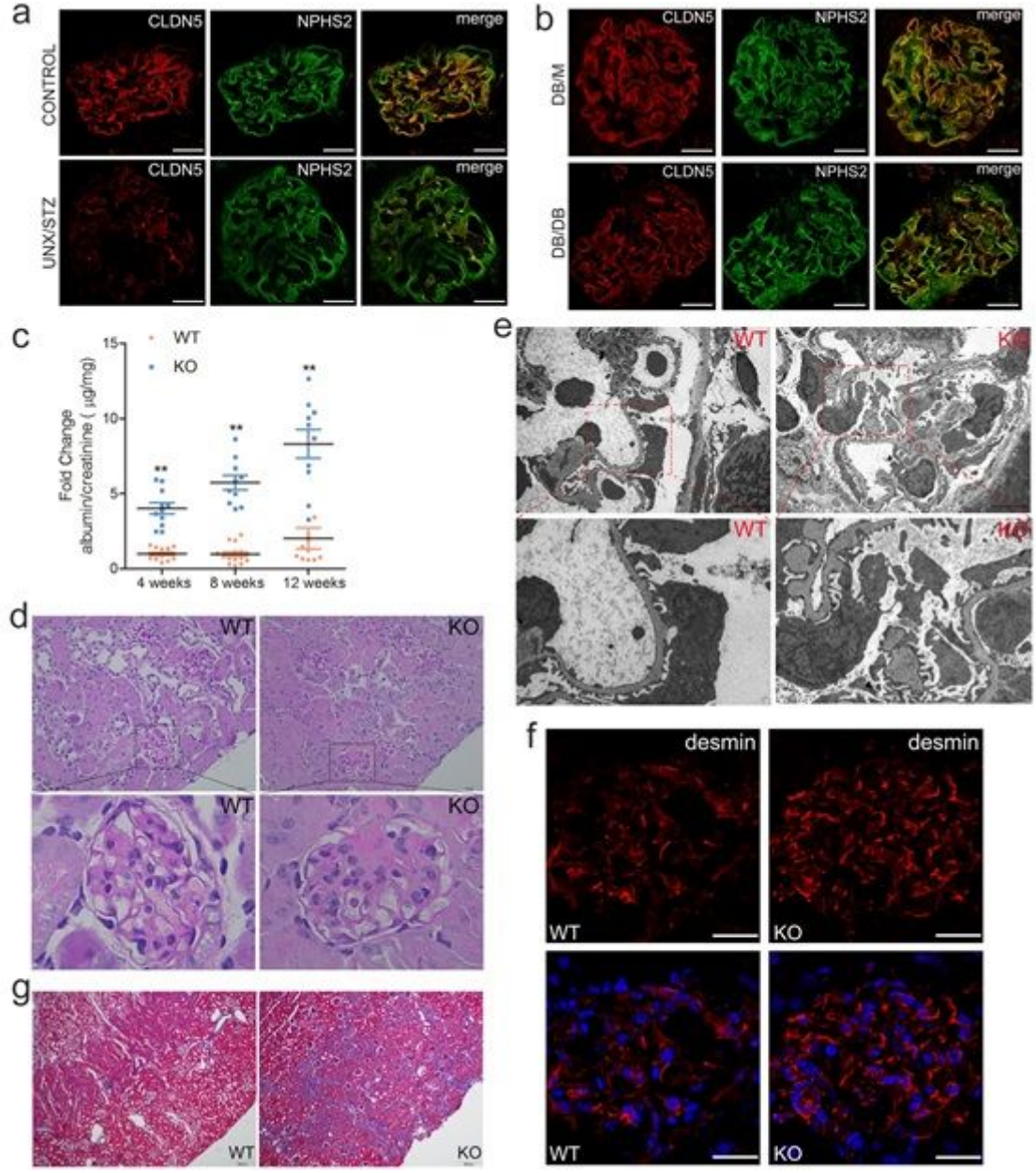

Figure 2

Podocyte-specific Cldn5 deletion mice show increased susceptibility to diabetic kidney injury. (a) Double immunostaining of CLDN5 (red) and NPHS2 (green) of kidney sections from control and DN (UNX/STZ) mice 12 weeks after the last injection of STZ. Scale bars, 20 μm. (b) Double immunostaining of CLDN5 (red) and NPHS2 (green) of kidney sections from control (DB/M) and DN (DB/DB) mice at 24 weeks of age. Scale bars, 20 μm. (c) Development of albuminuria (shown as fold change of the ratio of albumin to creatinine) after 4, 8 and 12 weeks of the last injection of STZ (n = 10, **P < 0.01). (d-e) Knockout of Cldn5 in podocytes induces development of nodular glomerulosclerosis with flattening of foot processes, as assessed by PAS staining (d) and electron microscopy (e) 12 weeks after the last injection of STZ, in comparison to WT controls. Scale bars for D, 50 μm. Scale bars for E, 2 μm. (f) Immunostaining of podocyte injury marker desmin of kidney sections from WT and Cldn5 KO DN mice 12 weeks after the last STZ injection. Nuclei were visualized by DAPI. Scale bars, 20 μm. (g) Masson's trichrome staining images of whole kidney showing interstitial fibrosis in Cldn5 KO diabetic mice 12 weeks after the last injection of STZ. Scale bars, 200 μm.

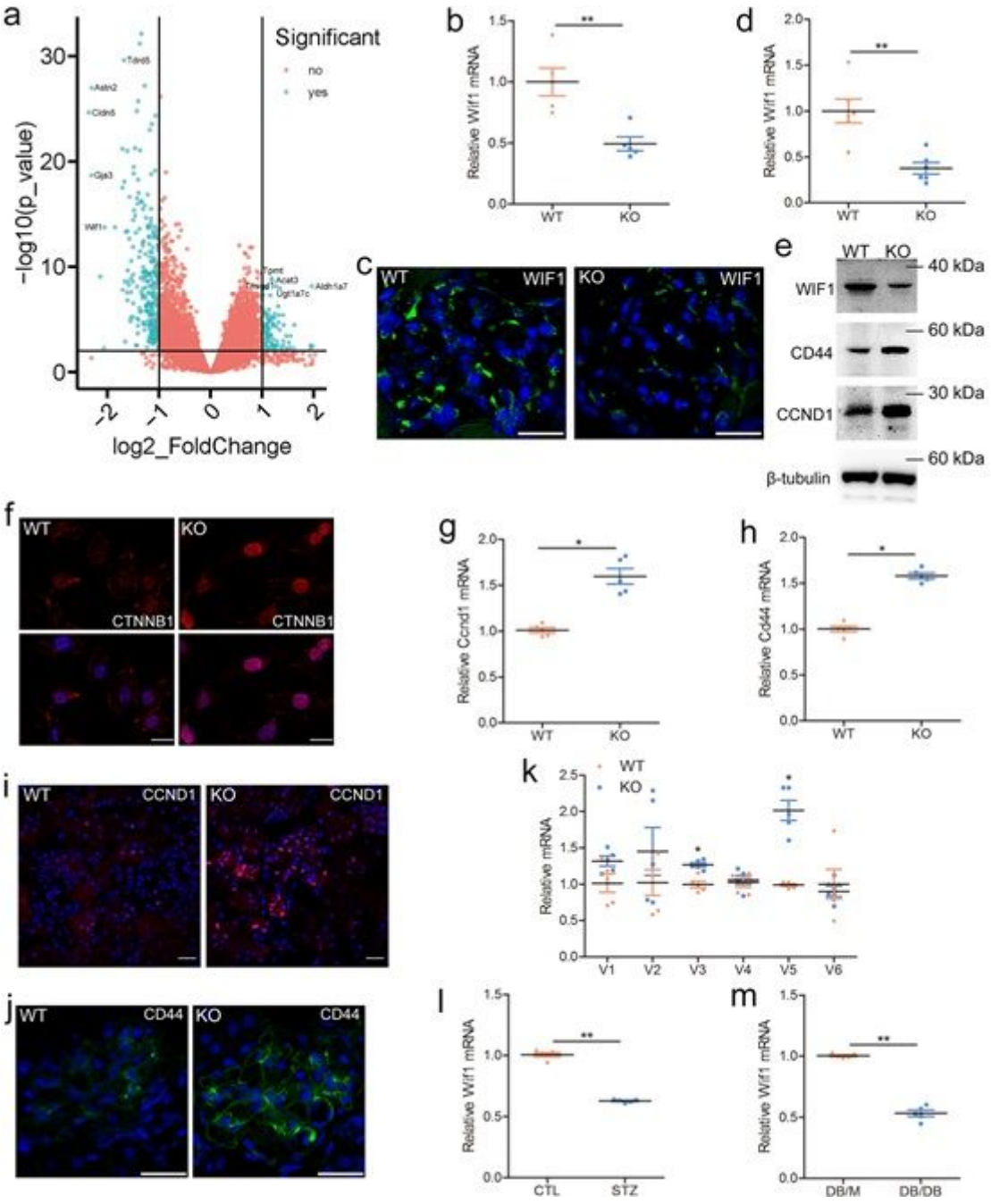

Figure 3

CLDN5 regulates WNT signaling pathway activity in podocytes through control the transcriptional expression of Wif1. (a) Differentially expressed genes (Cldn5podKO VS Cldn5ctrl) illustrated in a volcano plot (n = 5, fold change > 2, and P < 0.05). (b) Expression of Wif1 mRNA assessed by qRT–PCR in kidney from WT and Cldn5 KO mice (n = 5, **P < 0.01). (c) Representative images of immunofluorescence for WIF1 in kidney sections from WT and Cldn5 KO mice. (d) Expression of Wif1 mRNA assessed by qRT–PCR in glomerulus from WT and Cldn5 KO mice (n = 6, **P < 0.01). (e) Immunoblotting for WIF1 and WNT target genes (CD44 and CCND1) in isolated glomerulus from WT and Cldn5 KO mice. (f) Representative images of immunofluorescence for CTNNB1 in FACS-sorted podocytes from WT and Cldn5 KO mice. (g-h) mRNA expression of Ccnd1 (g) and Cd44 (h) assessed by qRT–PCR in isolated glomerulus from WT and

Cldn5 KO mice. (n = 5, *P < 0.05). (i-j) Immunofluorescence of CCND1 (i) and CD44 (j) in kidney sections from WT and Cldn5 KO mice. (k) mRNA expression of different isoforms of Cd44 assessed by qRT–PCR in isolated glomerulus from WT and Cldn5 KO mice (n = 5, *P < 0.05). (l) mRNA expression of Wif1 assessed by qRT–PCR in isolated glomerulus from control (CTL) and STZ-induced type I diabetic mice (STZ), 12 weeks after the last injection of STZ (n = 6, **P < 0.01). (m) mRNA expression of Wif1 assessed by qRT–PCR in isolated glomerulus from DB/M and DB/DB type 2 diabetic mice at 24 weeks of age (n = 6, **P < 0.01). Nuclei were visualized by DAPI. Scale bars, 20 μm.

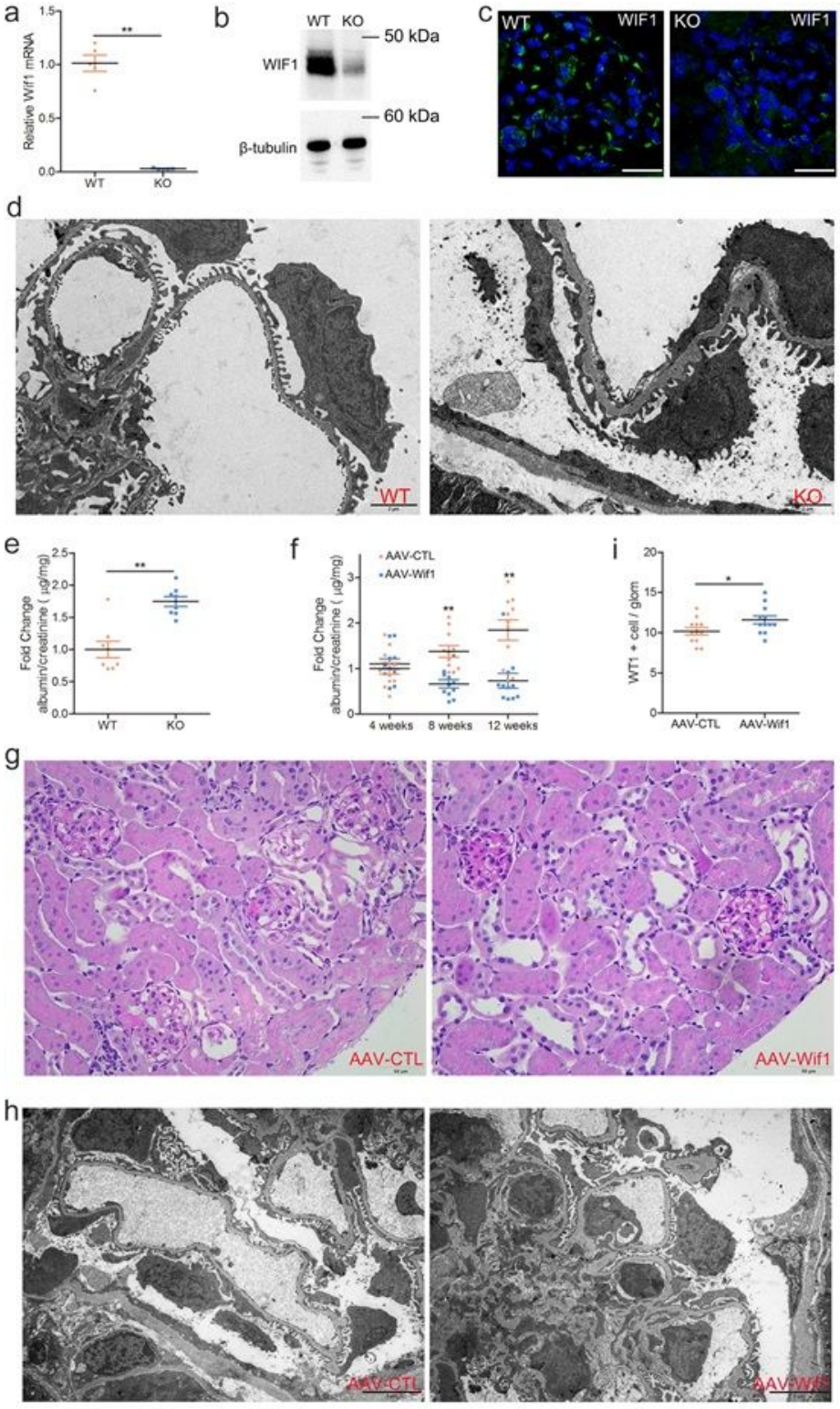

Figure 4

Podocyte specific Wif1 knockout (a-e) and overexpression (f-i) mice analysis. (a) qRT-PCR analysis in isolated glomerulus showing loss of Wif1 gene expression in Wif1 KO mice (n = 5, **P < 0.01). (b) Western blot analysis for WIF1 of isolated glomerulus from WT and Wif1 KO mice. (c) Immunofluorescence staining for WIF1 performed in WT and Wif1 KO mice. Nuclei were visualized by DAPI. Scale bar, 20 μm. (d) TEM images of glomerular capillary loops of 16-week-old WT and Wif1 KO mice. Scale bar, 2 μm. (e) Albumin-to-creatinine ratios (μg/mg) of spot urine samples of 16-week-old WT and Wif1 KO mice (n = 8 mice per group, **P < 0.01). (f) Albumin/creatinine ratio (μg/mg) in spot urine of AAV-CTL and AAV-Wif1 treated mice 4, 8 and 12 weeks after the last dose of STZ injection (n = 11, **P < 0.01). (g) Representative PAS-stained kidney images of AAV-CTL and AAV-Wif1 treated mice. Scale bar, 50 μm. (h) TEM images of glomerular capillary loops in AAV-CTL compared with AAV-Wif1 treated mice. Scale bar, 5 μm. (i) Quantification of WT1-positive cells in the AAV control (CTL) and AAV Wif1 (Wif1) treated mouse glomerulus (n = 6, *P < 0.05).

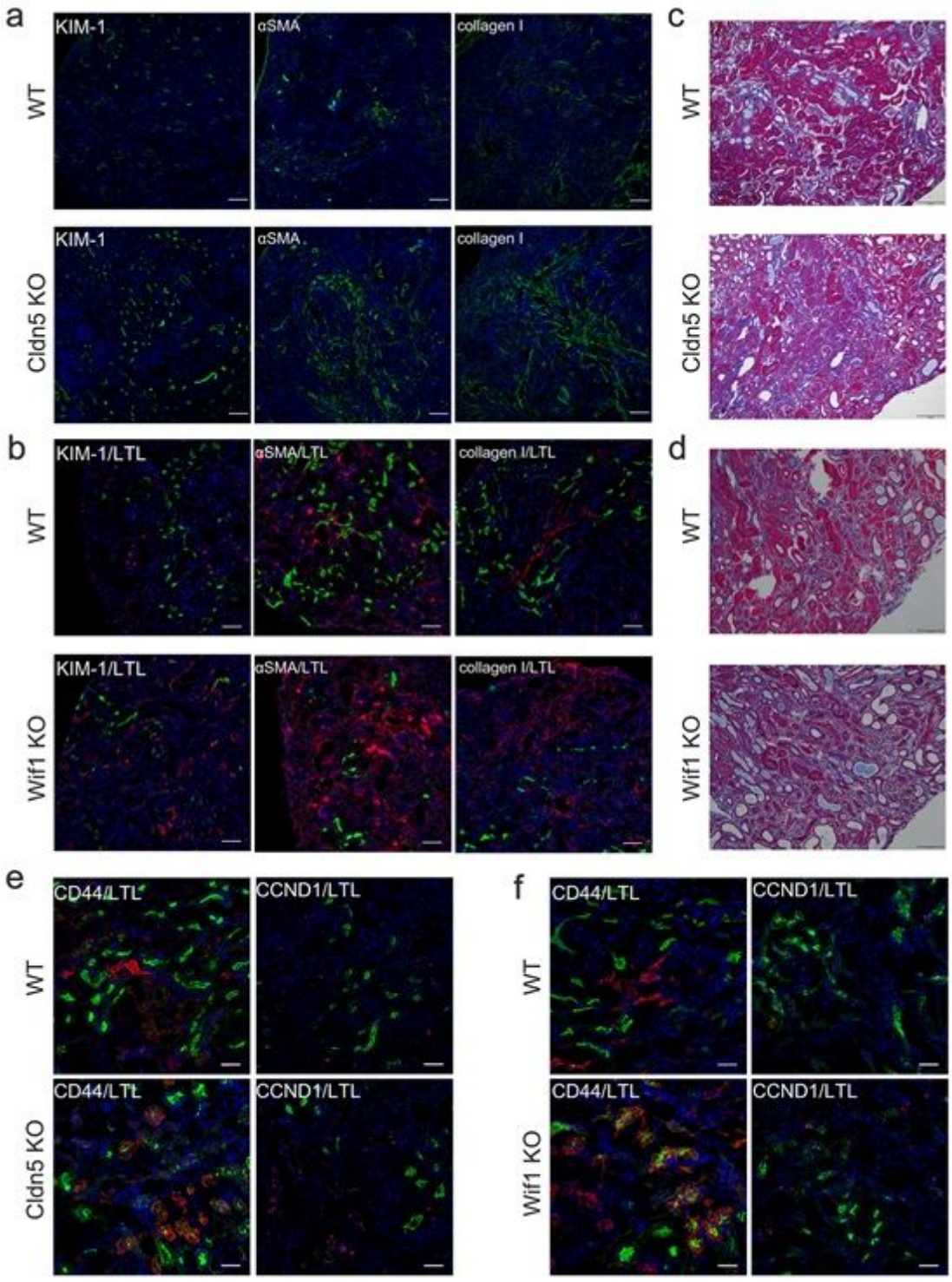

Figure 5

Podocyte-specific loss of CLDN5 or Wif1 exacerbates interstitial fibrosis in UUO mouse model. (a) Immunofluorescence for KIM1, αSMA and collagen I in kidney sections from WT and Cldn5 KO mice. Scale bar,100 μm. (b) Double immunofluorescence for KIM1 (red), αSMA (red) and collagen I (red) with LTL (green) in kidney sections from WT and Wif1 KO mice. Scale bar,100 μm. (c) Masson's Trichrome staining of kidneys from WT and Cldn5 KO mice. Scale bar,100 μm. (d) Masson's trichrome staining of kidneys from WT and Wif1 KO mice. Scale bar,100 μm. (e) Immunofluorescence for CD44 (red) and

CCND1 (red) in kidney sections from WT and Cldn5 KO mice. Scale bar, 20 μm. (f) Immunofluorescence for CD44 (red) and CCND1 (red) in kidney sections from WT and Wif1 KO mice. Scale bar, 20 μm. LTL (green) was used as a proximal tubule marker. Nuclei were visualized by DAPI.

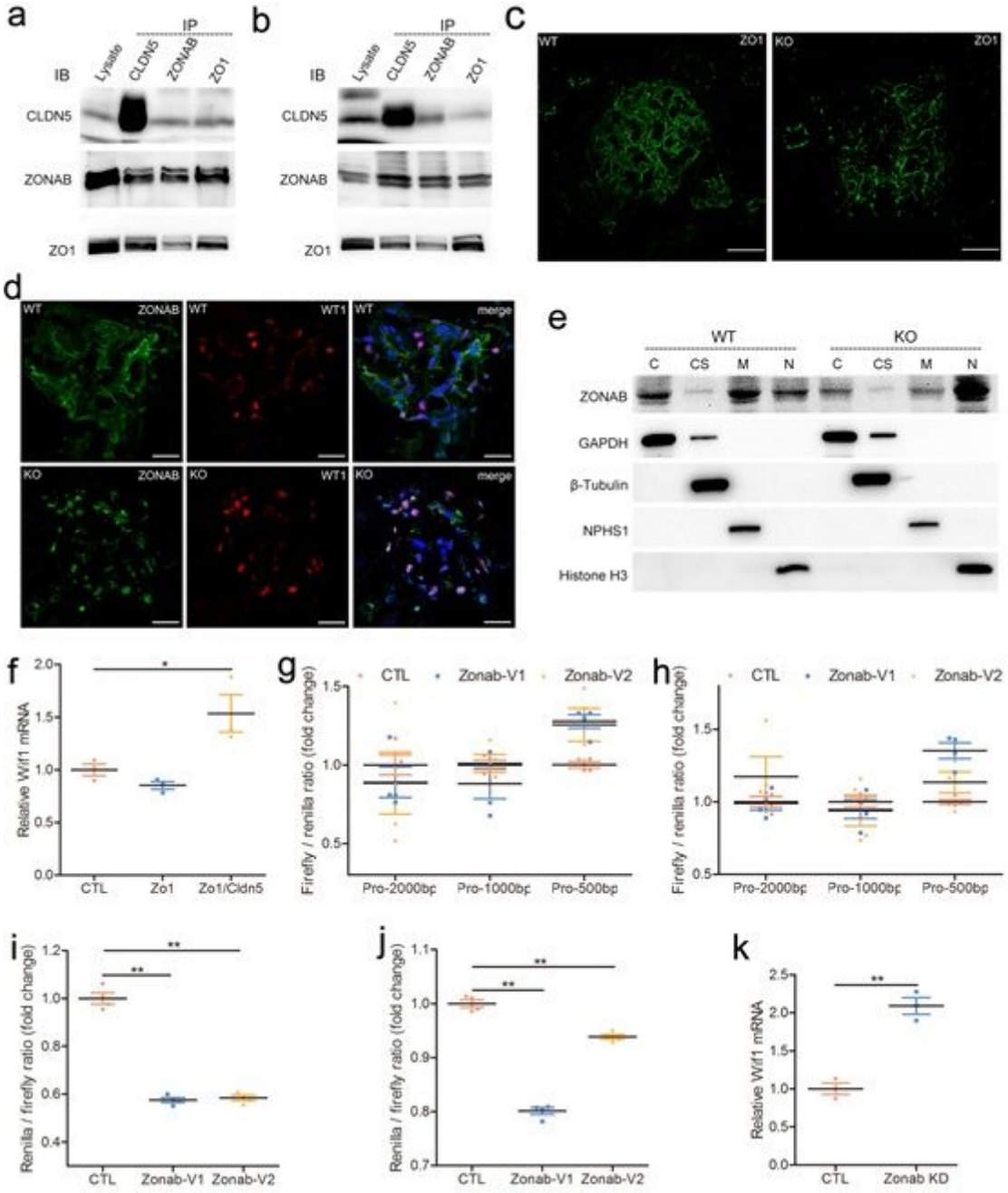

Figure 6

Regulation of Wif1 expression by CLDN5. (a) Co-IP of CLDN5, ZO1 and ZONAB in multiply transfected HEK293 to determine CLDN5 and ZO1/ZONAB interaction. (b) Co-IP experiments show that endogenous CLDN5 interacts with endogenous ZO1/ZONAB in isolated mouse glomerulus. Antibodies used for immunoprecipitation are shown above the lanes; antibody for blot visualization is shown at left. (c) ZO1 immunostaining in kidney sections from WT and Cldn5 KO mice. Scale bar, 20 μm. (d) Double immunostaining for ZONAB (green) and WT1 (red) in kidney sections from WT and Cldn5 KO mice. Nuclei were visualized by DAPI. Scale bar, 20 μm. (e) Western blot for ZONAB expression in the glomerulus of

WT and Cldn5 KO mice. Glomerulus were isolated from WT and KO mice followed by fractionation. The levels of ZONAB were analyzed by western blot, with GAPDH, β-tubulin, Nephrin, and Histone H3 serving as controls for the purity of the cytosolic fraction (C), cytoskeletal fraction (CS), membrane fraction (M) and nuclear fraction (N), respectively. (f) Expression levels for Wif1 mRNA in Cldn5 KO primary podocytes transfected with empty vector pcDNA3 (CTL), expression vector for Zo1, or co-transfected with expression vector for Zo1 and Cldn5 (n = 3, *P < 0.05). (g-h) Luciferase reporter activity of WIF1 promoter fragments in MDCK (g) and primary podocytes (h) transfected with empty vector pCMV6 (CTL), pCMV6-Zonab-V1, or pCMV6-Zonab-V2 (n = 4). (i-j) The Renilla/Firefly luciferase activity ratios measured in MDCK (i) and primary mouse podocytes (j) transfected with Wif1:3'-UTR and empty vector pCMV6 (CTL), pCMV6-Zonab-V1, or pCMV6-Zonab-V2 (n = 4, **P < 0.01). (k) Effects of transfection with siRNA for Zonab on Wif1 gene expression in primary podocytes from Cldn5 KO mice (n = 3, **P < 0.01).

Supplementary Files

This is a list of supplementary files associated with this preprint. Click to download.

- SupplementalNC.docx